Synthesis of monophasic $Ce_{0.5}Zr_{0.5}O_2$ solid solution by microwave-induced combustion method

Benjaram M. Reddy · Gunugunuri K. Reddy ·
Ataullah Khan · Ibram Ganesh

Abstract Nanocrystalline monophasic $Ce_{0.5}Zr_{0.5}O_2$ solid solution (1:1 molar ratio) has been synthesized by microwave-induced combustion method in a modified domestic microwave oven (2.45 GHz, 700 W) in approximately 40 min from cerium nitrate and zirconium nitrate precursors using urea as ignition fuel. For the purpose of better comparison, a $Ce_xZr_{1-x}O_2$ solid solution (1:1 molar ratio) was also synthesized by a conventional co-precipitation method from nitrate precursors and subjected to different calcination temperatures. The synthesized powders of both methods were characterized by means of X-ray powder diffraction, thermogravimetry/differential thermal analysis, scanning electron microscopy, and BET surface area techniques. Oxygen storage capacity (OSC) measurements were performed to understand the usefulness of these materials for various applications. The characterization results reveal that the sample obtained by microwave-induced combustion-synthesis route exhibits homogeneous monophasic $Ce_{0.5}Zr_{0.5}O_2$ solid solution whereas the co-precipitated sample displays compositional heterogeneity. The OSC measurements reveal that the materials synthesized by both methods exhibit comparable oxygen vacancy content (δ).

B. M. Reddy (✉) · G. K. Reddy · A. Khan
Inorganic and Physical Chemistry Division, Indian Institute
of Chemical Technology, Hyderabad 500 007, India
e-mail: bmreddy@iict.res.in

I. Ganesh
Centre for Silicon Carbide, International Advanced
Research Centre for Powder Metallurgy and New Materials
(ARCI), Balapur (PO), Hyderabad 500 005, India

Introduction

Ceria–zirconia solid solutions have been recognized as key materials for various applications ranging from catalysis [1–3], to ceramics [4], fuel cell technologies [5], and solid state electrolytes [6]. The addition of zirconia to the cubic structure of ceria increases oxygen storage capacity (OSC) while enhancing its thermal stability as compared to pure ceria alone, hence these oxide solid solutions were exploited extensively in the formulation of modern three-way-catalysis (TWC) for automotive exhaust purification [1, 2]. The technological applicability of $Ce_xZr_{1-x}O_2$ solid solutions is expanding very rapidly [1]. In view of their commercial significance various preparative routes were employed to make $Ce_xZr_{1-x}O_2$ solid solutions which include, precipitation [7], impregnation [8], precursor modification [9], sol–gel [10], surfactant-assisted [11], micro-emulsion [12], hydrothermal-solvothermal [13], ceramic [14], mechanical milling [15], spray pyrolysis [16], sputtering [17], and chemical vapor deposition [18]. It is a well-known fact in the literature that synthesis methodology and process conditions strongly influence the physicochemical properties of the resulting materials such as phase composition, crystallite size, surface area, redox ability, and OSC [1]. Also well-known that preparation methods like co-precipitation can lead to high specific surface area, however the temperature stability of these oxides is characterized by a severe loss of surface area at elevated temperatures. Further, the wet chemical routes require calcination at high temperatures for prolonged times which leads to crystallite growth and decrease in reactivity. Synthetic methodologies based on sol–gel and related routes require expensive precursors, such

as alkoxides. Also the atomic homogeneity of the materials obtained by these routes are rather poor although they exhibit controlled textural and surface properties [19]. Therefore, there are several attempts these days to develop an efficient and cost effective preparation methodology to obtain thermally stable and catalytically active $Ce_xZr_{1-x}O_2$ solid solutions for various applications.

Depending on the Ce/Zr atomic ratio and calcination temperature, three different phases (cubic, monoclinic or tetragonal) are frequently reported for $Ce_xZr_{1-x}O_2$ solid solutions [20, 21]. Cubic phase normally dominates in the ceria rich compositions, whereas monoclinic is predominant in the zirconia rich combinations. The metastable tetragonal phase exists in a wide composition range (5–80 mole % Ce) when different synthesis conditions are employed [20, 21]. Interestingly, the phase composition strongly influences the redox behavior of $Ce_xZr_{1-x}O_2$ solid solutions [20, 21]. These days there is a general agreement that the presence of a single-phase solid solution is preferable compared to micro-domain or phase segregated non-homogeneous CeO_2–ZrO_2 mixed oxides, as the former system generally leads to better textural stability and redox properties [1–3].

There is a growing interest in microwave processing of materials over conventional methods because of significant reduction in manufacturing cost, in terms of energy and time, better product homogeneity, and unique microstructures resulting in better physico-chemical properties [22–24]. The theory of microwave heating and the interaction of materials with the microwaves have been discussed elsewhere [25, 26]. As known the microwave heating is fundamentally different from conventional heating wherein the heat generates internally through material–microwave interaction instead of originating from an external heating source [27]. Combustion synthesis of materials can be performed very effectively using microwave energy [28]. Because of its novel internal heating mechanism, microwave energy heats the entire sample volume almost uniformly. The surface of the sample radiates energy, resulting in higher temperatures at the interior of the sample. Thus in microwave combustion, because of higher temperatures, the sample ignites in the center and a combustion wave front propagates outward in a radial manner. The primary objective of the present investigation was to explore the usefulness of microwave-assisted combustion method to synthesize homogeneous monophasic CeO_2–ZrO_2 solid solutions adopting the simple and cost-effective processing route. For the purpose of better comparison, an identical molar composition CeO_2–ZrO_2 solid solution

was also prepared by conventional co-precipitation method. Samples obtained by both methods were characterized by means of X-ray diffraction, BET surface area, thermogravimetry, scanning electron microscopy, and oxygen storage capacity measurements.

Materials and methods

Microwave-induced combustion synthesis

To synthesize $Ce_xZr_{1-x}O_2$ (1:1 molar ratio based on oxides) solid solutions by microwave-induced combustion method, cerium and zirconium nitrates were chosen as precursors since nitrates favor combustion. In a typical experiment, the requisite quantities of cerium(III) nitrate (Aldrich, AR grade) and zirconium(IV) nitrate (Fluka, AR grade) were dissolved separately in deionized water and mixed together in a Pyrex glass dish (150 × 80 mm). A stoichiometric quantity (as per the concept used in propellant chemistry) of solid urea (Fluka, AR grade) was added to the aforementioned mixture solution and stirred rigorously to obtain a clear solution. The dish containing the reaction mixture was introduced into a modified domestic microwave oven (BPL, India Limited, BMO-700T, 2.54 GHz, 700 W). Initially, the solution boils and undergoes dehydration followed by decomposition and spontaneous combustion with the evolution of large amounts of gases, including N_2, CO_2, and H_2O along with some small traces of NH_3 and NO_2 followed by a spontaneous flame resulting in a light yellow residual mass. The entire combustion process in the microwave oven took around 40 min to produce highly voluminous $Ce_xZr_{1-x}O_2$ powders. Three to four experiments were conducted under identical conditions to check for reproducibility. Properties of all the synthesized powders were found to be identical.

Co-precipitation

A $Ce_xZr_{1-x}O_2$ (1:1 mole ratio) solid solution was also prepared by a co-precipitation method with dilute ammonium hydroxide. In a typical experiment, the requisite quantities of ammonium cerium(IV) nitrate (Loba Chemie, GR grade) and zirconium(IV) nitrate (Fluka, AR grade) were dissolved separately in deionized water and mixed together. Dilute liquid ammonia solution was added drop-wise to the mixture solution with vigorous stirring until the precipitation was complete. The resulting precipitate was filtered off, washed with deionized water, oven dried at 383 K for

16 h, and calcined at 773 K for 5 h in air atmosphere. A small portion of this sample was once again calcined at 1,073 K for 5 h in a closed muffle furnace in air atmosphere.

Characterization techniques

The TG/DTA plots were obtained on a Mettler-Toledo TG-SDTA apparatus. Sample (ca. 15 mg) was heated from ambient to 1,273 K under nitrogen flow and the heating rate was 10 K min^{-1}. The BET surface areas were determined by N$_2$ adsorption at liquid nitrogen temperature using a Micromeritics Gemini 2360 Instrument. Prior to analysis, samples were oven dried at 393 K for 12 h and flushed with Argon gas for 2 h. X-ray powder diffraction patterns were recorded on a Bruker D8 diffractometer using nickel-filtered Cu K$_\alpha$ (0.15418 nm) radiation source. Crystalline phases were identified by comparison with the reference data from ICDD files. The average crystallite size of Ce$_x$Zr$_{1-x}$O$_2$ solid solution was estimated with the help of Scherrer equation [29]. High resolution scanning electron microscopy analyses were carried out with a Hitachi S-4300 (SE/N) microscope, operating at an accelerating voltage of 20 kV. The potential OSC was examined by oxygen release characteristics of the powders in the temperature range 573–1,073 K. The change in the weight of sample was monitored by thermogravimetry (TG) under cyclic heat treatments in flowing nitrogen and dry air. A commercial Netzsch (Luxx, STA, 409 PC, Germany) TG-DTA analyzer was employed for this purpose. The heat cycle consisted of heating the sample to 1,073 K in N$_2$, cooling down to 423 K in dry air, and again heating to 1,073 K in N$_2$ environment. All heating and cooling rates were 5 K min^{-1}. The weight loss of sample during the second heating cycle was used to measure the oxygen release properties (δ). This technique of OSC evaluation is essentially similar to that described previously [30–32].

Results and discussion

Combustion methods generally involve auto ignition of metal precursors containing an oxidizer (metal nitrate) and an organic fuel such as urea. The resulting materials characteristics such as surface area and crystallite size are strongly dependent on the fuel to oxidant ratio. The required stoichiometry between the metal nitrates and the urea was calculated using total oxidizing and reducing valences of the components as reported in the literature [33, 34]. Generally, the oxidizing and reducing valences s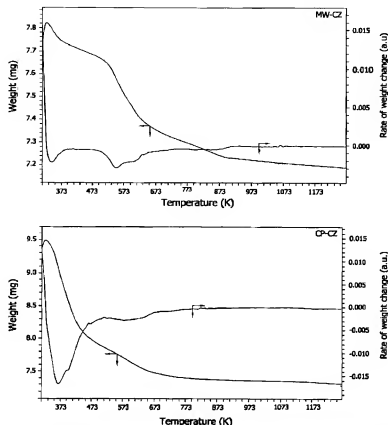erve as numerical coefficients for stoichiometric balance so that the equivalent ratio is close to unity and the energy released during the combustion will be maximum [33, 34]. According to the concepts used in propellant chemistry, the elements Ce, Zr, C, and H posses reducing valences of +3, +4, +4, and +1, respectively, and oxygen has an oxidizing valence of –2. The valence of nitrogen is zero [33, 34]. Thus, the oxidizing and reducing valences of Ce(NO$_3$)$_3$, Zr(NO$_3$)$_4$, and CO(NH$_2$)$_2$ become –15, –20, and +6, respectively. Thus the amount of urea (fuel) required in the process to yield maximum energy with 1:1 molar ratio metal precursors was estimated by balancing the following equation as reported previously [33–35]

$$1(-15) + 1(-20) + n(+6) = 0; \quad n = 5.83 \text{ mole urea.}$$

The combustion reaction of urea [CO(NH$_2$)$_2$ (C) + 1.5 O$_2$ (g) $\rightarrow$ CO$_2$ (g) + 2H$_2$O (g) + N$_2$ (g)] is exothermic [–129.9 kcal ($\Delta H°$, 298 K)] and supplies the adequate heat required for the completion of the powder synthesis reaction. The heat of formation [$\Delta H_f°$ (298 K)] of various components are as follows: CO(NH$_2$)$_2$ (C): –79.71 kcal mol^{-1}; CO$_2$ (g): –94.051 kcal mol^{-1}; H$_2$O (g): –57.796 kcal mol^{-1}; N$_2$ (g) and O$_2$ (g): 0, where (c) = crystalline, (l) = liquid, (g) = gas [36, 37]. The necessary prerequisite to initiate the combustion process is to expose the redox reaction mixture to higher temperatures of approximately 773 K in an electrical furnace or in the microwave oven. Water, urea, and nitrates of the precursors used possess permanent dipole moments and become heated when subjected to microwaves due to their continuous molecular rotations. Although nitrates, water, and urea exhibit some anisotropy with respect to the microwave interactions, the cumulative heat generated by the redox mixture as a whole is adequate to initiate the combustion process [22, 38]. Also due to the properties of internal and volumetric heating, thermal gradients during microwave processing are avoided, thereby providing a uniform environment for the reaction. The combustion process will be finished when all the flammable substances are burned out. Finally, it turns out to be a loose substance which shows voids, pores, and high friable formed by the escaping gases during the combustion reaction. The whole process takes less time to yield the powders of desired stoichiometry and composition.

The obtained Ce$_x$Zr$_{1-x}$O$_2$ samples of both microwave-induced combustion synthesis and co-precipitation method (before calcination) were subjected to TG analysis. The obtained thermograms, between 323 and 1,273 K, are shown in Fig. 1. As can be noted from Fig. 1, the TG profile of the microwave-combustion (MW) sample is different from that of the one obtained

Fig. 1 TG profiles of
$Ce_xZr_{1-x}O_2$ samples
obtained by microwave
combustion (MW) and
co-precipitation (CP) method

by co-precipitated (CP) method. In the case of MW sample, the first low temperature peak in the range 303–373 K is due to loss of adsorbed water on the surface of the sample. The other broad peak observed in the 493–633 K range could be attributed to the loss of residual nitrates and undecomposed urea. The first major low temperature peak in the range 323–463 K, in case of CP sample, is primarily due to the loss of non-dissociative adsorbed water as well as water held on the surface by hydrogen bonding. While the second minor weight loss peak in the 513–673 K range could be attributed to loss of water due to dehydroxylation of the surface as synthesized when synthesized through hydroxide gels. Interestingly, a nominal weight loss of 5.4% is observed for the MW synthesized sample, when compared to a 21.4% loss for the CP sample from ambient to 1,273 K last temperature investigated in this study. The N_2 BET surface areas of both samples are shown in Table 1. As can be noted from this table, the MW sample exhibits reasonably high specific surface area when compared to that of CP sample calcined at 1,073 K. The 773 K calcined CP sample exhibits more surface area as expected since its treatment temperature is less than that of the MW sample.

The X-ray powder diffraction patterns of various samples investigated in the present study are shown in
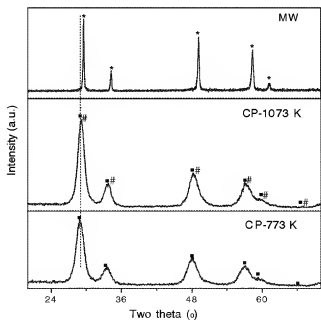
Fig. 2. As can be noted from this figure, formation of a single phase (monophasic) crystalline $Ce_{0.5}Zr_{0.5}O_2$ (PDF-ICDD 38-1436) has been confirmed from the XRD patterns of the MW sample. Additionally, the presence of sharp diffraction peaks signifies that the sample is predominantly in crystalline form. The XRD patterns of CP sample calcined at 773 and 1,073 K are also shown in Fig. 2. As can be noted, the CP sample calcined at 773 K exhibits poor crystallinity. Only the broad diffraction lines due to cubic fluorite type phase with the composition $Ce_{0.75}Zr_{0.25}O_2$ (PDF-ICDD 28-0271) are visible. With increasing calcination temperature an increase in the intensity of the lines due to better crystallization of this phase could be seen. A slight shift in the peak positions ($2\theta = 28.90–29.32$) with increasing calcination temperature could be noted which indicate that along with particle growth some compositional changes are also taking place. A detailed analysis of XRD patterns revealed the formation of additional $Ce_{0.6}Zr_{0.4}O_2$ phase (PDF-ICDD 38-1439) at 1,073 K calcination temperature as established in our earlier publication [39]. This is primarily due to a progressive increase of zirconium content into the ceria unit cell with increase of calcination temperature. Since the ionic radius of Zr^{4+} (0.84 Å) is smaller than Ce^{4+} (0.97 Å) incorporation zirconium ion into the ceria unit

Table 1 BET surface area, XRD phase, crystallite size and oxygen vacancy concentration (δ) measurements of $Ce_xZr_{1-x}O_2$ samples prepared by co-precipitation (CP) and microwave (MW) combustion

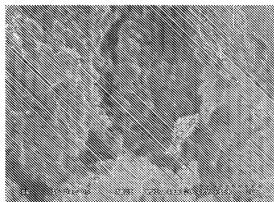| $Ce_xZr_{1-x}O_2$ sample	Surface area ($m^2\ g^{-1}$)	XRD phase	Crystallite size (nm)[a]	δ[b]
Co-precipitation				
773 K calcined	84	$Ce_{0.75}Zr_{0.25}O_2$	4.7	0.16[c]
1.073 K calcined	36	$Ce_{0.75}Zr_{0.25}O_2$; $Ce_{0.6}Zr_{0.4}O_2$	5.5	0.13
Microwave-induced combustion				
MW	56	$Ce_{0.5}Zr_{0.5}O_2$	45.4	0.12

[a] From Scherrer equation
[b] Determined by thermogravimetry. Under identical conditions pure CeO_2 exhibited 0.04
[c] Obtained in first cycle

cell leads to decrease of cell "a" parameter and shrinkage of the lattice [40]. It is obvious from the XRD results that the $Ce_xZr_{1-x}O_2$ solid solution is composed of different phases when obtained from co-precipitation method and tends to stabilize under the influence calcination temperature due to the phase segregation phenomenon as reported earlier by Kenevey et al. [41].

Fig. 2 X-ray powder diffraction patterns of $Ce_xZr_{1-x}O_2$ samples: (**a**) microwave combustion (MW) method; (**b**) co-precipitation (CP) method (calcinced at 773 and 1,073 K): (*) lines due to $Ce_{0.5}Zr_{0.5}O_2$; (■) lines due to $Ce_{0.75}Zr_{0.25}O_2$; (#) lines due to $Ce_{0.6}Zr_{0.4}O_2$

Crystallite size (D_{XRD}) of $Ce_{1-x}Zr_xO_2$ solid solutions in various samples as determined by X-ray line broadening technique is summarized in Table 1. As can be noted from Table 1 that the crystallite size depends on the method of preparation and the calcination temperature as well in the case of CP samples. The MW sample exhibits crystallite size more than that of the CP samples. It should be remembered that the particle size estimates of Ce–Zr solid solutions are subject to uncertainties attributed to the compositional non-uniformity. When using Scherrer equation, one assumes that the particle size effects are the only source of peak broadening. However, if compositional non-uniformity occurs in the particles, the particle size will be underestimated. A distribution of different zirconium concentrations within individual particles as well as between particles would lead to a distribution of two-θ values and thus broader peaks, which would be interpreted as, reduced particles using the Scherrer equation [41, 42].

Figures 3 and 4a, b represent the SEM micrographs of $Ce_{1-x}Zr_xO_2$ solid solutions obtained by microwave combustion and co-precipitation methods (773 and 1,073 K calcined), respectively. Interestingly, the MW sample exhibits uniform grain size and homogeneous distribution, while grains of various sizes could be noted in the case of CP samples. Further, an increase in the size of the particles could be noted (Figs. 4a, b) with increase of calcination temperature from 773 to 1,073 K in line with XRD observations. The potential OSC of the $Ce_xZr_{1-x}O_2$ solid solutions prepared by both methods was evaluated by thermogravimetry as per the procedure elaborated elsewhere [32]. The determined oxygen vacancy concentration or storage capacity (δ) pertaining to the samples are shown in Table 1. The parameter "δ" denotes the number of oxygen vacancies formed in the given sample under the

Fig. 3 SEM image of $Ce_xZr_{1-x}O_2$ sample prepared by microwave combustion (MW) method

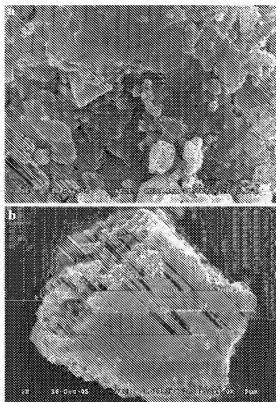**Fig. 4** (**a**) SEM image of Ce$_x$Zr$_{1-x}$O$_2$ sample prepared by co-precipitation (CP) method and calcined at 773 K. (**b**) SEM image of Ce$_x$Zr$_{1-x}$O$_2$ sample prepared by co-precipitation (CP) method and calcined at 1,073 K

microwave oven operated at 700 W and 2.45 GHz frequency. For comparison purpose, another same composition ceria–zirconia solid solution was also prepared by a co-precipitation method and subjected to different thermal treatments. Samples obtained by both methods were examined by means of XRD, TG, SEM, BET SA, and OSC measurements. The XRD results reveal formation of a well crystalline monophasic Ce$_{0.5}$Zr$_{0.5}$O$_2$ in case of MW sample and poorly crystalline Ce$_{0.75}$Zr$_{0.25}$O$_2$ and Ce$_{0.6}$Zr$_{0.4}$O$_2$ solid solutions in the case of CP sample calcined at 773 and 1,073 K, respectively. Further, sample obtained by MW method exhibits comparable specific surface area, crystallite size and oxygen storage capacity with that of CP samples. Therefore, microwave-induced combustion process can be treated as an effective powder synthesis route, which is simple, fast and most economical. In particular, this procedure does not require acids or bases to hydrolyze the corresponding salts and other subsequent steps like washing, filtration, drying, and calcination could be eliminated leading to the conservation of time and energy.

given set of experimental conditions employed. As can be noted from the table, both the samples exhibit reasonably higher OSCs when compared to pure CeO$_2$ alone, which exhibited a value of 0.04 under identical experimental conditions [32, 40]. The CP sample calcined at 773 K exhibited a slightly higher value than the MW sample. However, after few cyclic treatments the "δ" value was found to decrease due to increase in the crystallite size and phase stabilization on exposure to higher temperatures during OSC measurements. On the other hand the MW sample exhibited a stable and constant OSC even after several cycles. Generally, the smaller particles will have a low energy of reduction and exhibit more oxygen vacancy concentration. On the whole the MW sample shows stable monophasic Ce$_{0.5}$Zr$_{0.5}$O$_2$ solid solution with reasonably good specific surface area and oxygen storage capacity.

Summary

By adopting a simple microwave-induced combustion synthesis method, preparation of 1:1 mole ratio Ce$_{1-x}$Zr$_x$O$_2$ solid solution was undertaken in a domestic

References

1. Di Monte R, Kaspar J (2005) J Mater Chem 15:633 and references therein
2. Trovarelli A (2002) In: Hutchings GJ (ed) Catalysis by ceria and related materials, catalytic science series, vol 2. Imperial College Press, London
3. Bernal S, Kasper J, Trovarelli A (1999) Catal Today 50:173
4. Bocanegra-Bernal MH, De La Torre SD (2002) J Mater Sci 37:4947
5. Steele BCH (1999) Nature 400:619
6. Jurado JR (2001) J Mater Sci 36:1133
7. Sergent N, Lamonier JF, Aboukais A (2000) Chem Mater 12:3830
8. Bensalem A, Verduraz FB, Delamar M, Bugli G (1995) Appl Catal A: Gen 121:81
9. Adachi G, Imanaka N (1998) Chem Rev 98:1479
10. Overbury SH, Huntley DR, Mullins DR, Glavee GN (1998) Catal Lett 51:133
11. Terrible D, Trovarelli A, Llorca J, De Leitenburg C, Dolcetti G (1998) J Catal 178:299
12. Garcia MF, Arias AM, Jues AI, Belver C, Hungrfa AB, Conesa JC, Soria J (2000) J Catal 194:385
13. Hirano M, Kato E (1996) J Ceram Soc Jpn 104:958
14. Yashia M, Arashi H, Kakihana M, Yoshimura M (1994) J Am Ceram Soc 77:1067
15. De Leitenburg C, Trovarelli A, Zamar F, Maschio S, Dolcetti G, Llorca J (1995) J Chem Soc Chem Commun 2181
16. Mani TV, Varma HK, Damodaran AD, Warrier KGK (1993) Ceram Int 19:125

17. Izu N, Murayama N, Shin W, Matsubara I, Kanzaki S (2004) Japanese J Appl Phys Part 1 43:6920
18. Bui W, Choy KL, Stelzer NHJ, Scoonman J (1999) J Solid State Ionics 116:225
19. Yoldas BE (1993) J Sol-Gel Sci Technol 1:65
20. Fornasiero P, Di Monte R, Rao GR, Kaspar J, Meriani S, Trovarelli A, Graziani M (1995) J Catal 151:168
21. Sinev MY, Graham GW, Haach LP, Shelef M (1996) J Mater Res 11:1960
22. Mingos DMP, Baghurst DR (1991) Chem Soc Rev 20:1
23. Fu Y-P, Lin C-H (2003) J Alloys Compds 354:232
24. Ganesh I, Johnson R, Mahajan YR, Madhavendra SS, Reddy BM (2005) Ceram Inter 31:67
25. Sutton WH (1989) Am Ceram Soc Bull 68:376
26. Kiminami RHGA, Morelli MR, Folz DC, Clark DE (2000) Bull Am Ceram Soc 79:63
27. Clark DE, Amad I, Dalton RC (1991) Mat Sci Eng A 144:91
28. Clark DE, Sutton WH (1996) Ann Rev Mat Sci 26:299
29. Cullity BD (1978) Elements of XRD, 2nd edn. Addison-Wesley, Reading, MA
30. Ozawa M, Loong CK (1999) Catal Today 50:329
31. Logan AD, Shelef M (1994) J Mater Res 9:468
32. Reddy BM, Khan A, Lakshmanan P, Aouine M, Loridant S, Volta JC (2005) J Phys Chem B 109:3355
33. Merzanov AG (1993) Int J Self-Propagat High Temp Synth 2:113
34. Patil KC, Aruna ST, Ekambaram S (1997) J Curr Opin Solid State Mater Sci 2:158
35. Ganesh I, Johnson R, Mahajan YR, Khan A, Madhavendra SS, Reddy BM (2004) J Mater Res 19:1015
36. Dean JA (ed) (1979) Lange's handbook of chemistry 12th edn. McGraw-Hill, New York
37. Lide DR (ed) (1993) CRC hand book of chemistry and physics, 73rd edn. CRC Press, London, UK
38. Rao KJ, Ramesh PD (1995) Bull Mater Sci 18:447
39. Reddy BM, Khan A, Lakshmanan P, Loridant S, Cartes CL, Rojas TC, Fernandez A (2005) J Phys Chem B 109:13545
40. Reddy BM, Khan A (2005) Catal Surveys Asia 9:155
41. Kenevey K, Valdivieso F, Soustelle M, Pijolat M (2001) Appl Catal B: Environ 29:93
42. Reddy BM, Khan A, Yamada Y, Kobayashi T, Loridant S, Volta JC (2003) Langmuir 19:3025